SAND2000-2894C

THE EFFECT OF CHLORINE IMPLANTATION ON THE PITTING BEHAVIOR OF ALUMINUM

F. D. Wall, J. C. Barbour, J. P. Sullivan, N. Missert, B. Bunker, G. Nelson
Sandia National Laboratories
Albuquerque, NM 87185-0340

ABSTRACT

Using plasma-beam techniques, an engineered Al oxide has been placed on Al thin film substrates. Electrochemical testing indicates that this structure has a low susceptibility to pitting corrosion making it an ideal control on which to study the impact of intentionally introduced defects. Results from potentiodynamic polarization experiments and chemical etching indicate that this engineered oxide is extremely robust compared to air-formed oxides. Subsequent ion beam implantation was used to introduce Cl into the deposited oxide. Minimal impact on both electrical and ionic conductivity of the oxide was observed for Cl concentrations of approximately 0.4 a/o. Approximately an order of magnitude higher Cl concentration is expected in an oxide formed after HNO_3 etching to the peak of the Cl implant distribution. This oxide had an elevated ionic conductivity and enhanced susceptibility to pit initiation.

INTRODUCTION

It is generally accepted that pit initiation in high purity Al takes place at a local defect in the protective oxide or over a heterogeneity in the underlying material. It is extremely difficult to determine the nature of the interactions that lead to pit initiation because of the small size scale over which these processes occur. A methodology for potentially overcoming this difficulty is to modify the bulk behavior of the metal or oxide and correlate changes in pitting behavior to the nature of the modifications. Many researchers have used ion implantation into the substrate material, followed by natural oxidation as a means of modifying the oxide behavior [1-12]. Instead of relying on the natural oxidation of the Al metal, our approach is to engineer oxides that have much reduced defect density compared to native oxides. Defects can then be intentionally introduced and the impact on pitting behavior determined using conventional electrochemical techniques. In this work, plasma-beam techniques were used to deposit artificial amorphous aluminum oxides, and ion implantation was used to introduce chlorine defects into the oxide.

EXPERIMENTAL

Thin film sample preparation

Al films were deposited on SiO_2/Si substrates that were then coated with a thin deposited alumina layer and implanted with Cl^+ ions. Samples were grown using

DISCLAIMER

electron beam evaporation of aluminum at 0.1 nm/s to a thickness of approximately 180 nm. Upon completion of the Al deposition, a thin alumina layer was formed using electron beam evaporation of Al at 0.1 nm/s and co-bombardment with O_2^+ ions from an electron cyclotron resonance (ECR) plasma. The deposition chamber base pressure was $0.4\text{-}1\text{x}10^{-8}$ Torr and during alumina deposition an O_2 flow rate of 2.5 sccm produced a background O_2 pressure of $5\text{-}7\text{x}10^{-5}$ Torr O_2. The ions in the ECR plasma were generated using 100 Watts of 2.45 GHz microwave power and a magnetic field of 875 Gauss, forming the ECR resonance condition upstream from the deposition chamber. The O_2^+ ions in the ECR plasma have a mean energy of approximately 30 eV when impinging upon a sample at the floating potential. Some samples were implanted at room temperature with 35 keV Cl^+ ions to a fluence of $1\text{x}10^{16}$ Cl/cm^2. The ions were incident at an angle of 5° relative to the surface normal. The fluence was chosen to produce a level of damage in the sample such that near the surface in the oxide layer each atom was displaced approximately 2 times, and well into the Al layer, at a depth of 100 nm, each atom was displaced approximately 10 times. Figure 1 shows the calculated [13] Cl profile after implantation. The maximum concentration of Cl in the oxide layer is ≈ 0.4 at. % and at a depth of 36 nm into the Al the peak concentration of Cl was almost 4 at. %.

Electrical measurements

Samples for electrical measurement were prepared by patterning Au contacts with areas ranging from ~ 2×10^{-7} cm^2 to 4×10^{-4} cm^2 on to the Al oxide surface. The most frequently used contact size was 2.5×10^{-5} cm^2 in area (a square contact 50 μm by 50 μm). The Au contacts were fabricated by electron beam deposition under high vacuum onto photolithographically patterned photoresist covered samples followed by a lift-off procedure. Electrical characterization was performed on capacitor (metal-insulator-metal) structures using the Au top contact as one electrode and the Al layer beneath the oxide as the bottom electrode. The DC electrical measurements included current-voltage sweeps (between ~ -1 V to +1 V) followed by sweeps to higher potentials (typically a few volts either positive or negative) until dielectric breakdown occurred. Measurements were performed at room temperature with a sweep rate of approximately 5 to 10 mV/sec and an instrumental noise level of 10 fA. The AC electrical measurements included capacitance-frequency and AC conductance-frequency sweeps over the frequency range of 1 Hz to 1 MHz. The frequency sweep was completed in approximately 10 minutes.

Electrochemical testing

Electrochemical experiments were performed in either 50% HNO_3 or 0.05 M NaCl (pH ~ 6.5) at 25°C. Three-electrode electrochemical impedance spectroscopy (EIS) was performed using a 10 mV RMS AC waveform superimposed on a 0 V vs. open circuit DC potential. Three-electrode potentiodynamic polarization experiments were run following either an open circuit exposure or a potentiostatic hold at –0.950 V_{SCE} (details will be reported with the data in the *results* section). Scan rates used included 1 mV/s and 0.1667 mV/s. Some of the samples were tested using the repetitive polarization scan (RPS) technique that was described in detail elsewhere in these proceedings [14]. Briefly, the RPS approach uses multiple scans in a single experiment to measure multiple pitting potentials.

Secondary ion mass spectroscopy

Secondary ion mass spectroscopy (SIMS) analysis was used to generate depth profiles for species found within the Al oxide. The experiments were performed using a 16 keV Ga ion beam for sputtering and analysis. The sputtered area was 90 μm by 90 μm and the analysis area was 25 μm by 25 μm. Detected ions generally included Cl^-, F^-, O^-, AlO^-, O_2^- and OH^-. Details of SIMS analysis can be found elsewhere [15].

RESULTS

Electrochemical and electrical properties of deposited Al oxide

Potentiodynamic polarization testing of evaporated Al with a 50 Å deposited oxide in 50 mMol NaCl resulted in pitting potentials ranging from +0.1 to +1.5 V_{SCE} (Fig.2). A typical E_{pit} value for an air formed oxide on high purity (99.9999%) Al in this environment is around -0.680 V_{SCE} [16]. The increase in E_{pit} is a clear indication of the robustness of the deposited oxide. A second comparison of the deposited oxide to an air formed oxide was made by chemically etching samples in 50% HNO_3. The impedance and open circuit potential (E_{oc}) of the samples were monitored to determine the time until the oxide was completely dissolved. The polarization resistance (R_p) was observed to decrease, then reach a steady state of approximately 1000 Ω-cm^2. The steady state condition was taken as an indication that the original oxide had been dissolved and the impedance of the system represented equilibrium between oxide formation and oxide dissolution. The deposited oxide remained intact up to 7000 s whereas the air formed oxide (on 99.999 Al) dissolved is less than 1000 s of exposure (Fig 3). Once again, the superior resistance of the deposited oxide is clearly demonstrated.

The behavior of the deposited oxide was also probed using dry electrical measurements (Fig. 4). The leakage current is several orders of magnitude lower for the deposited oxide than for the air formed oxide indicating lower electrical conductivity and a lower defect density. Furthermore, the breakdown field (not shown) is higher for the deposited oxide suggesting that higher overpotentials may be required to induce pitting under aqueous conditions.

The effect of chloride implantation on the behavior of deposited Al oxide

As shown in Fig. 1 the implantation profile of chlorine is calculated to have a maximum value of 0.4 a/o Cl in the Al oxide. SIMS analysis was used to verify the implant profile (Fig. 5). The sputter efficiency for Cl in the oxide appears to be greater than that for Cl in the Al metal, resulting in a profile different from that shown in Fig. 1. Nevertheless, the SIMS data qualitatively indicate successful Cl loading of the oxide. Dry electrical measurements performed on control and implanted samples showed little effect of ion implantation on either leakage current or breakdown potential (Fig. 6). In contrast, potentiostatic polarization at –0.950 V_{SCE} in 50 mMol NaCl showed an increase in oxide conductivity corresponding to Cl implantation (Fig. 7). Despite this increase in conductivity, only a slight difference in pitting behavior was indicated by the

potentiodynamic polarization data (Fig. 8). Most notably, the ranges of pitting potentials overlap for the control and implanted oxides.

Pitting characteristics of oxides formed in HNO_3

In order to examine an oxide with a higher level of Cl, the implanted samples were etched in 50% HNO_3 to dissolve the outermost 30-40 nm of sample and form an oxide at the peak of the Cl implant profile. Although the etch rate was calibrated to be between 30 Å/min and 40 Å/min, the final depth of etching was approximate. Follow-up SIMS data are being collected to document the distribution of Cl in the oxide and in the underlying metal. Control samples were prepared by etching non-implanted samples to remove approximately the same amount of material. For these samples the oxides are formed in the oxidizing HNO_3 environment and should bear no memory of the previously deposited oxide. Preliminary impedance data (Fig. 9) and polarization scans (Fig. 10) for the control and implanted samples indicate that the chlorine implantation results in a lower R_p value and enhanced metastable pitting.

DISCUSSION

The deposited oxide has excellent resistance to both electrochemical and chemical attack (Figures 2 and 3 respectively), making it an excellent platform on which to study intentionally introduced defects. Ion implantation was used to introduce Cl into the oxide at a maximum oxide concentration of approximately 0.4 a/o. The dry electrical properties showed no dependence on implantation at this level (Fig. 4) whereas electrochemical current flow at cathodic potentials showed a slight dependence (Fig. 7). Only a minor impact on pitting potential could be discerned (Fig 8). In contrast, when the level of Cl in the oxide was increased by etching further into the implant profile, both low frequency impedance and polarization behavior were strongly affected. The EIS data (Fig. 9) show a drop in R_p value from 86 $k\Omega\text{-}cm^2$ to 1.2 $k\Omega\text{-}cm^2$ with Cl implantation, indicating increased ionic conductivity in the oxide. From the polarization data (Fig. 9) it appears that there may be a slight increase in passive current density and a decrease in E_{pit} for the implanted sample. The most profound difference in the polarization behavior is the presence of anodic current fluctuations throughout the data for the implanted sample (Fig 10). These fluctuations are believed to represent metastable pitting and represent a significant difference in the susceptibility to pit initiation as a function of Cl incorporation into the oxide.

Other researchers have also investigated the impact of incorporated anions on oxide properties and pitting behavior [17-22]. Pryor et al. observed no change in high frequency impedance data for incorporation of Cl into anodic aluminum oxide but did report decreases in low frequency resistivity [17-19]. They explained these results as Cl increasing ionic conductivity but having no impact on electrical conductivity. The dry electrical measurements in this study are a direct measure of electrical conductivity and compare favorably with the results reported by Pryor. However, to date, the dry measurements have only been performed on the low Cl level oxide and interpretation should be confined to oxides containing no more than 0.4 a/o Cl. Our preliminary results on the oxide having a Cl content potentially greater than 0.4 a/o support Pryor's data that show enhanced ionic conductivity with the incorporation of Cl.

The impact of Cl defects on oxide conductivity suggests there should be an impact on pitting susceptibility. Skeldon et al. used both ion implantation [21] and electropolishing [22] to provide a source for incorporation of Cl during anodic growth of aluminum oxides. The primary intent of these studies was to identify the conditions necessary for Cl migration in the alumina. However, in the course of anodizing samples that contained incorporated Cl, evidence was found for metastable pitting in a chloride-free environment. Interestingly, their implantation was performed at a fluence of approximately 10^{15} ions/cm^2, whereas in the current study the fluence was 10^{16} ions/cm^2. Yet the polarization data (E_{pit}) presented here show no impact of ion irradiation. The apparent discrepancy may stem from the choice of environment. In the present case the environment (50 mMol NaCl) contains significant chloride and may mask the influence of low levels of ion implantation. The sample having the heightened level of Cl in the oxide did demonstrate elevated levels of metastable pitting vs. the control sample. In this case, perhaps, the level of oxide loading is sufficient to control the response of the sample even in a chloride-containing environment.

The evidence for metastable pitting in the implanted sample is the fluctuating current observed during the anodic polarization scan [Fig 10]. Likewise, the absence of fluctuations in the current for the non-implanted sample is interpreted as a lower occurrence of metastable pitting. It should be recognized that metastable pitting may be occurring in the non-implanted sample but is not detected due to either too slow of data acquisition rate or masking of the fluctuations due to too high of passive current density. Nevertheless, the implanted sample either has a higher occurrence of metastable pitting or when a metastable pit initiates it grows to a much larger size before repassivation occurs. If the former is the case then the Cl level in the oxide lowers resistance to pit initiation. If the latter is true, it implies that the Cl may modify the stability of the oxide such that when a pit initiates, more damage occurs before repassivation takes place. Future experiments using microelectrodes should separate these two effects and provide more conclusive results.

SUMMARY

1. A robust engineered aluminum oxide was produced using plasma beam techniques. It has superior chemical and electrochemical resistance than air-formed aluminum oxides while having approximately the same thickness. This engineered oxide / thin-film structure is a useful substrate on which to study intentionally introduced defects.

2. Implanting up to 0.4a/o Cl into the engineered oxide had little or no impact on electrical conductivity, ionic conductivity and pitting potential for the deposited Al oxide.

3. A Cl content of roughly 2 a/o in aluminum oxide formed in 50% HNO_3 caused an increase in ionic conductivity and an increase in susceptibility to metastable pitting.

REFERENCES

1. P. M. Natishan, E. McCafferty, G. K. Hubler, J. Electrochem. Soc., Accelerated Brief Communication, 1061-1062 (May, 1986).
2. P. M. Natishan, E. McCafferty, G. K. Hubler, J. Electrochem. Soc., V 135, no 2, 321-327 (1988).
3. W. C. Moshier, G. D. Davis, J. S. Ahearn, H. F. Hough, J. Electrochem Soc., Accelerated Brief Communication, 1063-1064 (May, 1986).
4. W. C. Moshier, G. D. Davis, J. S. Ahearn, H. F. Hough, J. Electrochem Soc., V134, no 11, 2677-2684 (1987).
5. W. C. Moshier, G. D. Davis, G. O. Cote, J. Electrochem. Soc., Vol. 136, No. 2, pp. 356-362 (Feb, 1989).
6. G. D. Davis, W. C. Moshier, T. L. Fritz, G. O. Cote, J. Electrochem. Soc., Vol. 137, No. 2, pp. 422-427 (Feb., 1990).
7. G. D. Davis, W. C. Moshier, G. G. Long, D. R. Black, J. Electrochem. Soc., Vol. 138, No. 11, pp. 3194-3199 (Nov., 1991).
8. B. A. Shaw, T. L. Fritz, G. D. Davis, W. C. Moshier, J. Electrochem. Soc., Vol. 137, No. 4, pp. 1317-1318 (April, 1990).
9. B. A. Shaw, G. D. Davis, T. L. Fritz, B. J. Rees, W. C. Moshier, J. Electrochem. Soc., Vol. 138, No. 11, pp. 3288-3295 (Nov., 1991).
10. G. D. Davis, B. A. Shaw, B. J. Rees, M. Ferry, J. Electrochem. Soc., Vol. 140, No. 4, pp. 951-959 (April, 1993).
11. G. S. Frankel, M. A. Russak, C. V. Jahnes, M. Mirzamaani, V. A. Brusic, J. Electrochem. Soc., Vol. 136, No. 4, pp. 1243-1244 (April, 1989).
12. G. S. Frankel, R. C. Newman, C. V. Jahnes, M. A. Russak, J. Electrochem. Soc., Vol. 140, No. 8, pp. 2192-2197 (Aug., 1993).
13. TRIM92, computer code by J. F. Ziegler, IBM Yorktown Heights, NY 14853.
14. F. D. Wall, M. A. Martinez, "Using Microelectrodes To Determine The Availability And Behavior Of Pit Initiation Sites In Aluminum", these proceedings.
15. B. C. Bunker, G. C. Nelson, K. Zavadil, J. C. Barbour, F. D. Wall, J. P. Sullivan, to be submitted to J. Phys. Chem. B. (2000).
16. J. R. Galvele, S. M. De Micheli, Proc. of the Fourth International Congress on Metallic Corrosion, Norman E. Hamner, Ed., NACE, Houston, TX, pp. 439-447 (1972).
17. J. J. McMullen, M. J. Pryor, "The Relation Between Passivation, Corrosion, and the Electrical Characteristics of Aluminum Oxide Films", Proceedings of the 1st International Congress on Metallic Corrosion, pp. 52-61, Butterworths (1961).
18. M. A. Heine, D. S. Keir, M. J. Pryor, J. Electrochem. Soc., Vol. 112, No. 1, pp. 24-32 (Jan, 1965).
19. A. F. Beck, M. A. Heine, D. S. Keir, D. Van Rooyen, M. J. Pryor, Corrosion Science, Vol. 2, pp. 133-145 (1962).
20. V. Ashworth, W. A. Grant, A. R. Mohammed, R. P. M. Procter, "The Effect of Ion Implantation on the Aqueous Corrosion Behavior of an Austenitic Stainless Steel", Ion Implantation Metallurgy, C. M. Preece and J. K. Hirvonen, eds., proc. AIME Symposium, Nov. 30, 1979, pp. 47-64.
21. M. Skeldon, K. Shimizu, P. Skeldon, G. E. Thompson, G. C. Wood, Corrosion Science, Vol. 37, No. 9, pp. 1473-1488 (1995).
22. K. Shimizu, G. M. Brown, K. Kobayashi, P. Skeldon, G. E. Thompson, G. C. Wood, Corrosion Science, Vol. 41, pp. 1835-1847 (1999).

This work was supported by the DOE Office of Basic Energy Sciences (BES). Sandia is a multiprogram laboratory operated by Sandia Corp., a Lockheed Martin Co., under U.S. DOE contract DE-AC04-94AL85000.

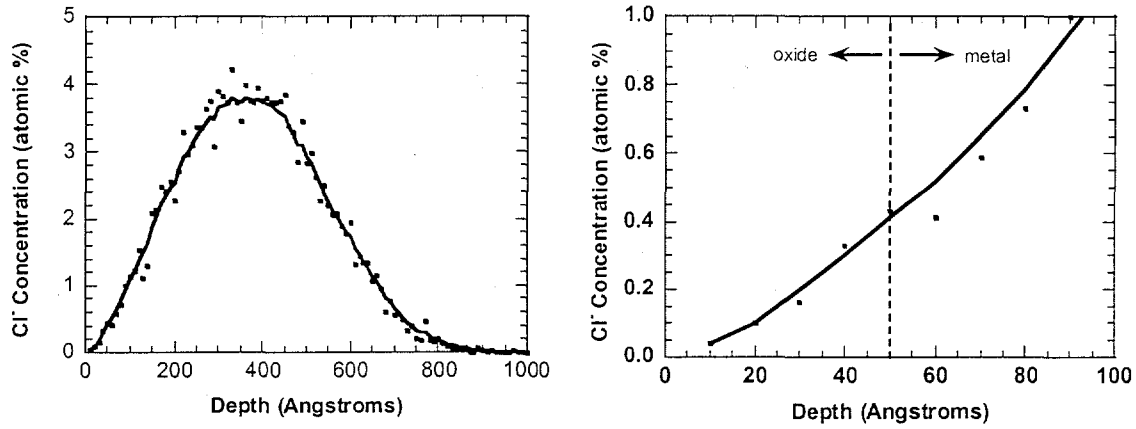

(a) (b)

Figure 1. Predicted Cl implant profile. (a) Maximum [Cl] occurs at about 360Å into the sample. (b) Peak [Cl] in the oxide is approximately 0.4 a/o.

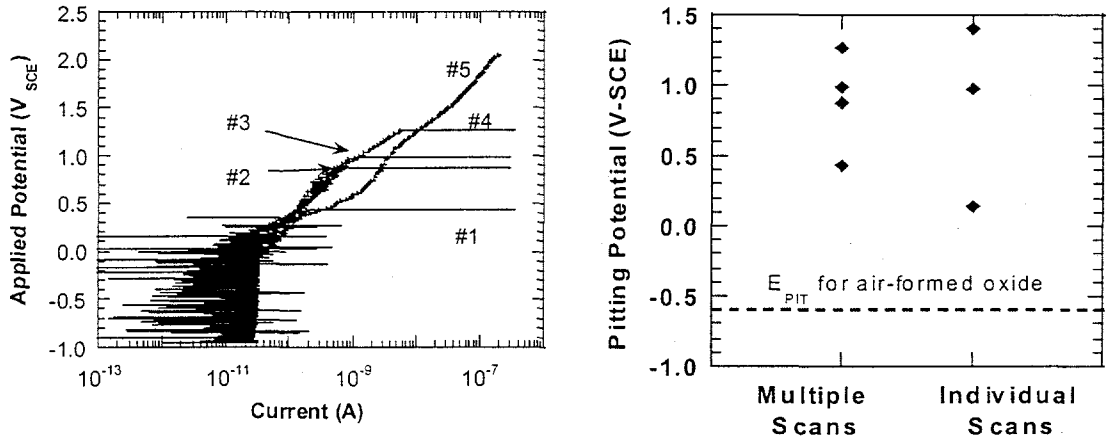

(a) (b)

Figure 2. Potentiodynamic polarization testing of ECR deposited oxide on Al thin film in 50 mMol NaCl, open to air, 25°C. (a) Raw data from repetitive polarization scan (dV/dt = 1mV/s). (b) Pitting potentials from 'a' together with pitting potentials from individual scans (dV/dt = 0.1667mV/s). The deposited oxide shows elevated resistance to pitting compared to data for air-formed oxides.

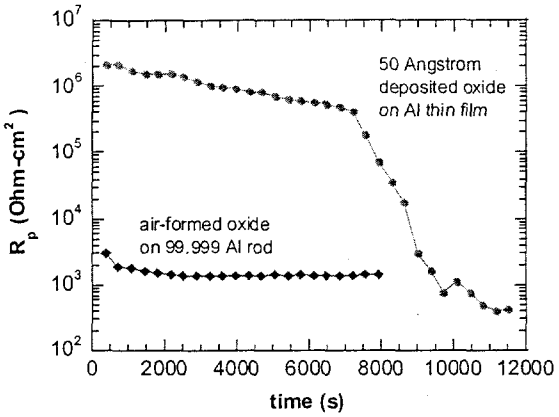

Figure 3. Effect of oxide exposure to 50% HNO_3. The air-formed oxide dissolves in less than 1000 s while the deposited oxide takes over 7000 s.

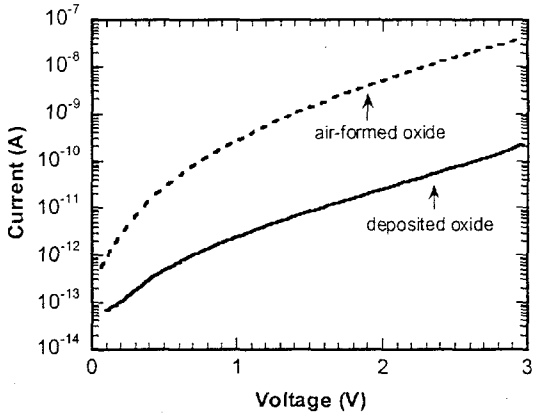

Figure 4. Conductivity of oxides tested using dry electrical measurements. The deposited oxide has a lower leakage current compared to the air-formed oxide indicating fewer electronic defects.

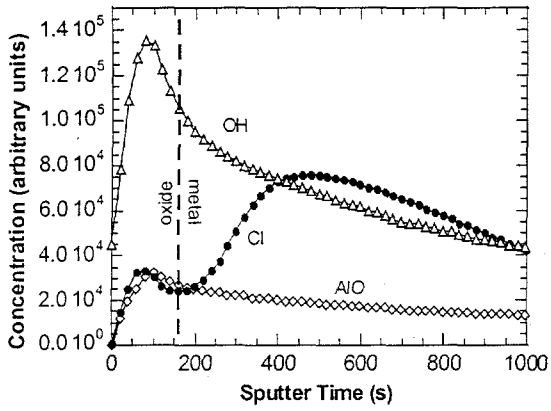

Figure 5. SIMS data showing implantation profile of Cl in thin film specimen. The peak in the oxide may be due to higher sputter efficiency in the oxide vs. in the metal. The tail in the OH and AlO data may be due to insufficient vacuum in the SIMS chamber.

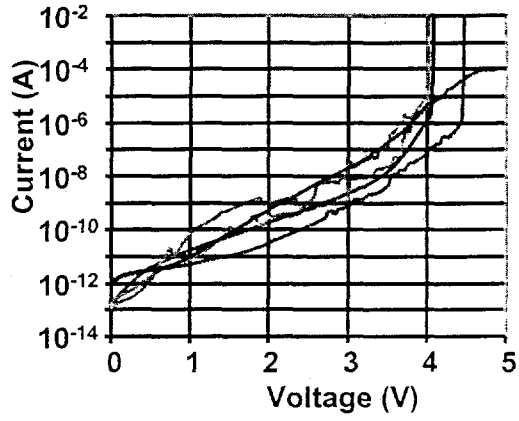

Figure 6. Dry electrical measurements show little impact of Cl ion implantation on leakage current and breakdown field. Data include un-implanted control, implanted sample, implanted + 12-hour exposure to deionized water.

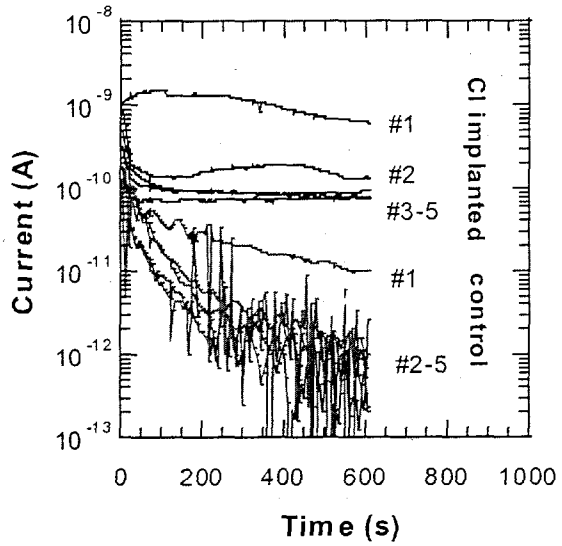

Figure 7. The effect of Cl loading in the oxide on cathodic polarization. Cathodic current during potentiostatic holds is higher for the Cl implanted oxide than the control. These data indicate a higher electronic conductivity and are not in agreement with the dry electrical measurements.

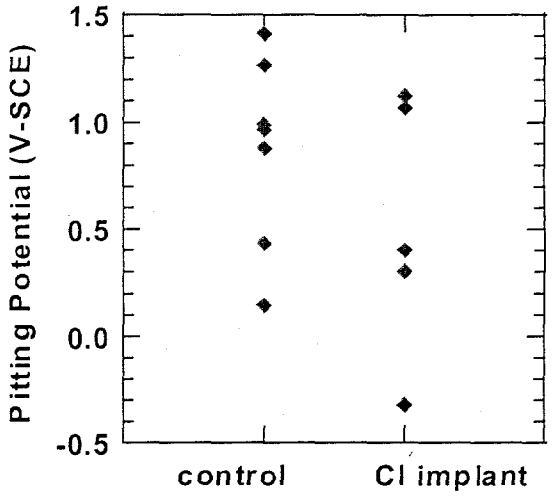

Figure 8. Effect of Cl implantation on pitting potential. The implant had a maximum Cl concentration in the oxide of 0.4a/o. This level does not appear to be sufficient to dramatically impact pitting potential.

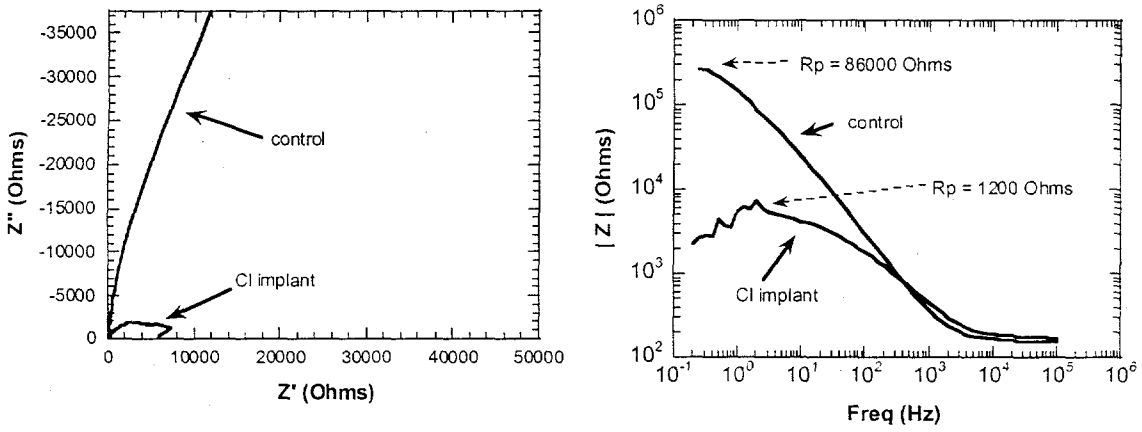

(a) (b)

Figure 9. EIS data comparing Cl implanted Al to control. Samples were etched in 50% HNO_3 in an attempt to maximize the Cl loading in the oxide by dissolving down to the peak in the implant profile. Implanted Cl appears to have a significant impact on polarization resistance. (a) Nyquist plot, (b) Bode magnitude plot. Samples were immersed in 50 mMol NaCl open to the air @ 25°C.

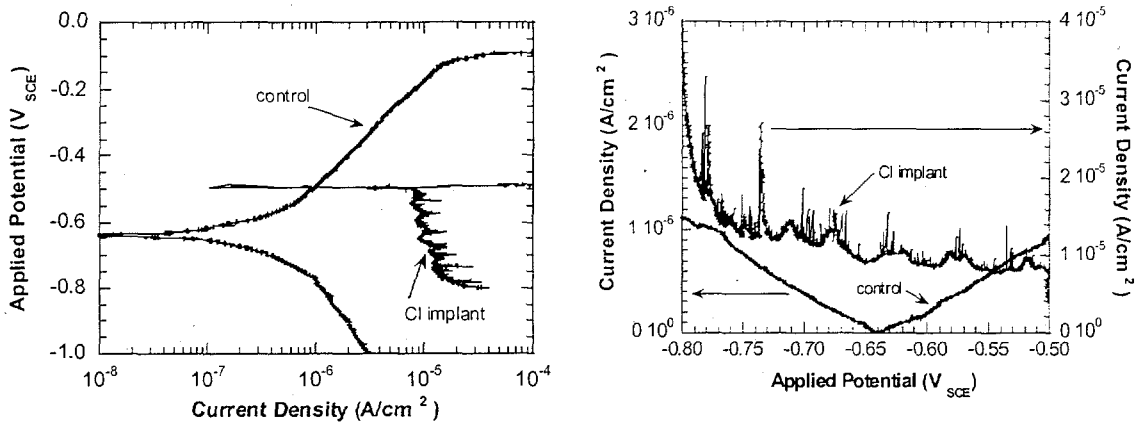

(a) (b)

Figure 10. Potentiodynamic polarization data comparing Cl implanted Al to unimplanted Al. Samples were etched in 50% HNO_3 in an attempt to maximize the Cl loading in the oxide by dissolving down to the peak in the implant profile. Implanted Cl appears to have a significant impact on metastable pitting. (a) Potential scan data, (b) Close-up of current data comparing lack of metastable pitting in control to high frequency of metastable pitting in Cl implanted sample. Scan rate was 0.1667 mV/s. Samples were immersed in 50 mMol NaCl open to the air @ 25°C.